buildings

MDPI

Article

# Multi-Criteria Decision Framework for Optimal Robotic System Selection in 3D Concrete Printing

**Ciprian Lapusan [1,2], Camelia Maria Negrutiu [2,3] and Ioan Sosa [2,3,*]**

[1] Department of Mechatronics and Machine Dynamics, Faculty of Automotive, Mechatronics and Mechanical Engineering, Technical University of Cluj-Napoca, 400114 Cluj-Napoca, Romania
[2] European University of Technology, European Union
[3] Department of Structures, Faculty of Civil Engineering, Technical University of Cluj-Napoca, 400114 Cluj-Napoca, Romania
* Correspondence: ioan.sosa@dst.utcluj.ro

**Abstract**

3D Concrete Printing (3DCP) is increasingly used for both on-site building fabrication and off-site production of structural components in controlled environments. The differences between these application contexts pose distinct requirements and constraints for the robotic systems used for material deposition. Selecting an appropriate robotic architecture, therefore, represents a critical design decision that directly influences printing quality and system performance. To address this challenge, this study proposes a multi-criteria decision-making framework for optimal selection of the robotic architecture for a 3DCP system, in accordance with its application requirements and constraints. For this, the method integrates AHP and TOPSIS, and takes into consideration factors such as technical characteristics, operational requirements, and economic costs. To demonstrate the applicability of the method, a case study was conducted to identify the most suitable robotic architecture for a laboratory-scale façade printing 3DCP system. Three robotic configurations were analyzed: a gantry system, an articulated robotic arm, and a parallel delta robot. The results showed that the articulated robotic arm achieves the highest TOPSIS closeness coefficient ($CC_i$ = 0.681), outperforming the other two configurations. These findings align with existing façade-oriented 3DCP studies and indicate that articulated robotic arms are well-suited for the fabrication of geometrically complex components with higher surface quality and dimensional accuracy. The results show that the proposed framework enables transparent, application-driven decisions during early-stage robotic system design for 3DCP.

**Keywords:** 3D concrete printing; robotic system architecture; multi-criteria analysis; optimal robotic system



Academic Editor: Muxuan Tao

Received: 4 November 2025
Revised: 23 December 2025
Accepted: 26 December 2025
Published: 2 January 2026



## 1. Introduction

In 2020, the construction sector accounted for almost 13% of the global GDP, with expenditures that exceeded $11 trillion [1]. This highlights the sector's central role in the global economy across both industrialized and emerging regions. However, the rapid demand for new buildings, particularly in fast-growing urban areas, has placed considerable pressure on the environment. Embodied emissions in the sector account for 10% of the global $CO_2$ emissions [2]. Construction-related waste has also become a major concern worldwide. In parallel with these environmental challenges, the construction industry is experiencing a persistent shortage of skilled labor, particularly in developed economies.

Juricic et al. [3] report an almost linear increase in construction job vacancies in the EU over the last decade. This trend was driven largely by the retirement of experienced professionals and the insufficient entry of younger workers into the industry. These workforce constraints, combined with the pressure to reduce the environmental footprint, have accelerated interest in alternative construction approaches. 3DCP is one promising direction, which has the potential to improve efficiency and sustainability in the field and, at the same time, unlock new possibilities in design and customization [4,5].

3DCP introduces a new construction method that automates the concrete placement process through layer-by-layer printing, reducing or eliminating the need for conventional formwork and associated on-site labor [6]. 3DCP also enables the production of geometrically complex and customized designs that are difficult or impossible to achieve with conventional techniques. At the structural level, 3DCP has been applied to print walls, load-bearing elements, and entire houses. In prefabrication, the technology is used to produce façade panels, bridge components, and other complex geometries that are difficult to achieve with conventional formwork. Beyond functional construction, 3DCP is increasingly used for customized and aesthetic applications, such as urban furniture, landscape features, and artistic installations [7]. The life-cycle assessments developed by Mohammad et al. [8] indicated that this technology has the potential to reduce $CO_2$ emissions by up to 30% and shorten construction time by 50–90%. This delivers improvements in efficiency and sustainability compared to traditional methods [9,10]. Furthermore, 3DCP is increasingly regarded as a promising solution for affordable housing and disaster relief due to its speed of construction and cost-effectiveness [11].

A key challenge in the development of 3DCP systems lies in the wide range of deployment contexts. The operational requirements are quite different across on-site and off-site environments [12]. In the case of on-site constructions, the systems must adapt to uneven terrain, variable weather conditions, and the logistical complexities of large-scale building projects [13–15]. In contrast, off-site prefabrication in controlled environments focuses on precision, repeatability, and integration with existing manufacturing workflows [16,17].

Developing the right system that can perform effectively for the specific scenario represents an important task. Cabibihan et al. highlighted this issue in [18]. They proposed a taxonomy and decision-making workflow as a first step toward creating a structured framework for selecting 3D printing technologies in construction. The paper concludes that addressing this issue is essential to progress beyond experimental projects (proof-of-concept). Even though 3DCP is advancing rapidly, there are still no established methods for selecting the right type of robot for different construction tasks. Currently, decisions about whether to use robotic arms, gantry systems, cable-driven setups, or hybrid configurations are often made on a case-by-case or ad hoc basis. In many cases, the decision is based more on what is available or convenient than on critical evaluation. This absence of a structured approach makes it difficult to objectively compare topologies. As a result, projects may underperform if the chosen robotic system does not align well with the specific demands of the construction task.

In this context, the objective of this study is to develop a multi-criteria framework for selecting optimal robotic architecture during the design of 3DCP systems that can be applied for both on-site and off-site applications. The proposed method combines the Analytic Hierarchy Process (AHP) and Technique for Order Preference by Similarity to Ideal Solution (TOPSIS) to systematically evaluate alternative robotic topologies. The framework integrates evaluation criteria related to the technical requirements, operational conditions, and cost considerations of the designed robotic system. This allows researchers and engineers to align the design choices with performance targets and resource allocation for an optimal solution. The framework is validated through a case study that identifies the most suitable robotic architecture for a laboratory-scale 3DCP system for façade printing.

The rest of the paper is structured as follows. Section 2 reviews the 3D concrete printing process, commonly used robotic architectures, and relevant MCDM approaches in robotics. Section 3 presents the proposed multi-criteria decision-making framework based on the integration of AHP and TOPSIS. Section 4 illustrates the application of the framework through a case study and discusses the obtained results. Section 5 concludes the paper by summarizing the main findings and outlining directions for future research.

## 2. Literature Review and Theoretical Background

### *2.1. Three-Dimensional Concrete Printing Technology*

3DCP is an additive manufacturing technique used in the construction industry that implements extrusion-based processes to deposit layers of cement material through a nozzle following a predefined pattern. Unlike conventional 3D printers designed for plastics, 3DCP systems present distinct characteristics due to the unique properties of cement-based materials and the specific demands of construction applications.

Besides the robotic framework that positions the extruder, these systems incorporate components that prepare and transport the printing material [6]. A typical 3DCP system is formed from multiple subsystems as schematically presented in Figure 1. The material storage (1) and mixing units (2) prepare the printing material mixture by blending cement, aggregates, water, and additives to achieve the required properties. The pumping (3) and delivery system transfers the material to the extrusion head (5). At the deposition stage, the extrusion nozzle shapes and lays down the material (7) layer by layer in accordance with the digital model.

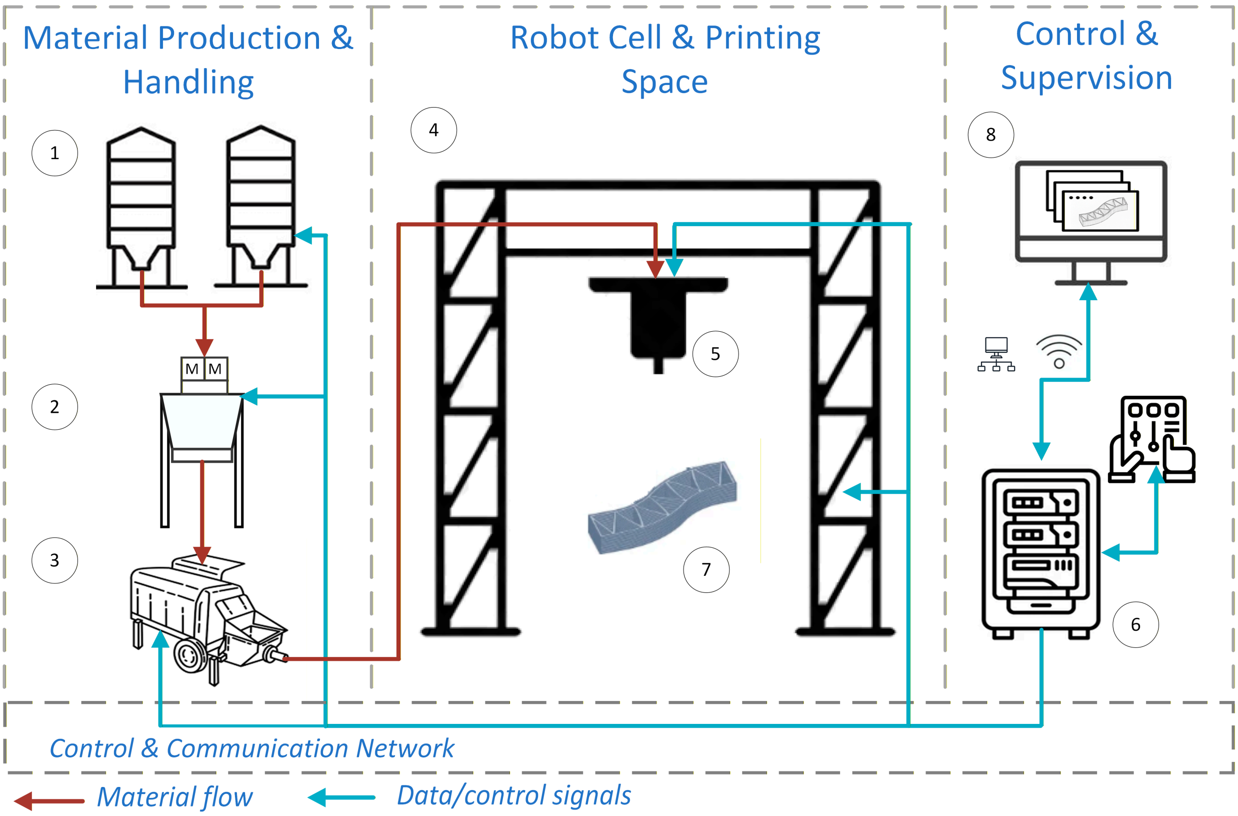


**Figure 1.** Schematic representation of a 3DCP system.

The robotic system (4) manages the spatial movement of the nozzle, typically using robotic arms, gantry setups, or hybrid solutions. The control system (6) integrates software and sensors to manage the printing process, to monitor material flow, to adjust parameters in real time, and to ensure precision. It uses the digital model of the printed object (8) to define executable machine commands. In this paper, the robot cell and printing space are addressed; the proposed method aims to identify the optimal robotic architecture for a given application.

### *2.2. Robotic Architectures Used for 3DCP Systems*

The robotic systems used in 3DCP must be capable of operating reliably under the demanding conditions of concrete printing. Unlike traditional robotic applications (e.g., manufacturing), 3DCP involves handling heavy materials, maintaining continuous extrusion, and maintaining good accuracy under varying loads and large workspaces. The most used robotic architectures include gantry-based systems, robotic arms, or parallel robots. Each of these topologies offers different advantages in terms of scalability, flexibility, and precision [19,20]. Recent research has also explored hybrid approaches, for example, integrating robotic systems with automated mixing and reinforcement placement to expand the scope of printable structures [4]. Next, the most used such platforms are presented.

Gantry systems, also known as Cartesian robots, are the most widely adopted platforms in 3DCP. Such a system consists of linear actuators arranged along orthogonal axes (Ox, Oy, Oz) (Figure 2a), resulting in decoupled motion that greatly simplifies the path planning (no singularity in the workspace) and control strategies. Gantry systems offer a large, well-defined workspace with high positional accuracy, making them suitable for on-site building-scale applications [21]. However, they lack flexibility in handling complex geometries due to a limited number of Degrees of Freedom (DoF) (typically 3 DoF).

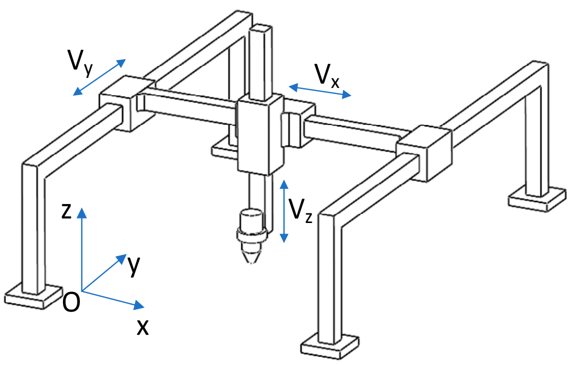


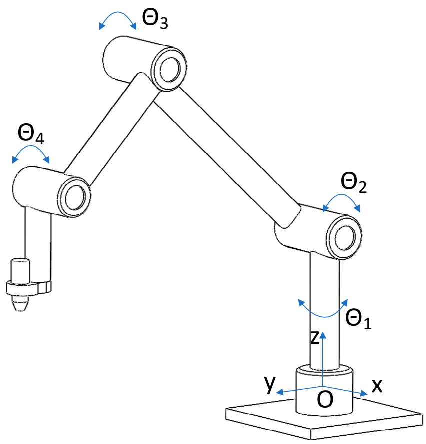


**Figure 2.** Robot architectures used in 3DCP: (**a**) schematic representation of a Cartesian robot (**b**) schematic representation of a robotic arm.

Articulated Robotic Arms (Figure 2b) consist of multiple kinematic elements connected in series using rotational joints (also, prismatic joints can be used, but are less common). Such robots are typically characterized by five or six DoF, providing higher flexibility and maneuverability, which enables printing of more complex and non-planar geometries [22]. Their workspace is typically spherical or toroidal in shape, which results in a smaller effective workspace volume compared to gantry systems with the same overall dimensions. Path planning is more complex due to the necessity to ensure avoidance of arm self-collision or singularities. They are particularly suited for prefabrication and customized components, where dexterity and nozzle orientation control are more important than the workspace scale.

Parallel robots, like the Delta robot, integrate multiple parallel kinematic links that control the end-effector pose (Figure 3a). These structures offer high speed, rigidity, and precision. These robots offer the smallest effective workspace for a given overall dimension compared with the previous two topologies. The kinematic and path planning are more complex and have smaller amplitudes in the orientation of the nozzle in comparison with articulated arms. While they are less common in large-scale 3DCP, they hold potential for high-accuracy printing of smaller or prefabricated elements [20].

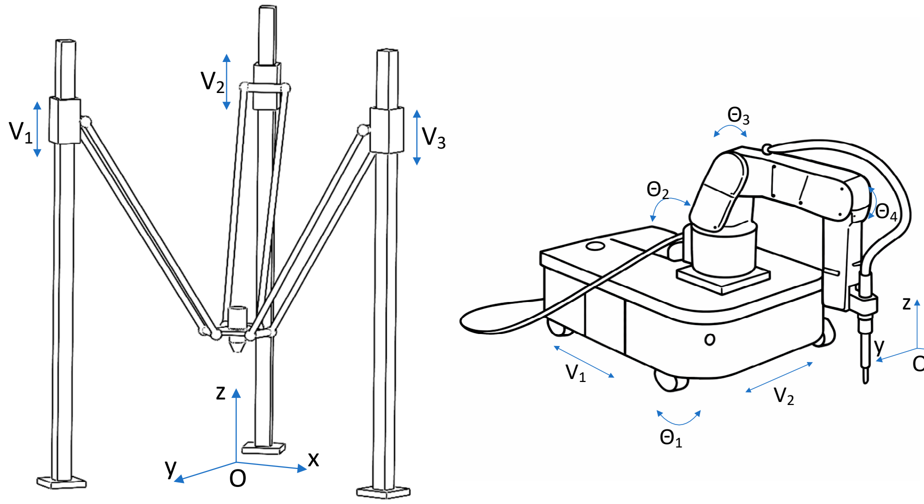


(a) (b)

**Figure 3.** Robot architectures used in 3DCP: (**a**) schematic representation of a parallel robot (**b**) schematic representation of a mobile platform with a robot arm.

Mobile robots with integrated arms combine mobility with robotic manipulation (Figure 3b) [23,24]. Mounting a robotic arm on a mobile base increases its effective workspace and enables adaptable on-site printing. The mobile system can navigate construction sites and extend the print area beyond fixed workspaces. However, this approach introduces additional complexity in control and system reliability, requiring precise localization, stability management, and motion coordination between the mobile base and the manipulator.

There are also other alternative configurations, such as cable-driven parallel robots [25] or hybrid systems that have been proposed to extend the printing area while reducing structural mass. These systems offer large workspaces at relatively low cost but face challenges in precision, control complexity, and robustness under variable loading conditions.

### *2.3. Multi-Criteria Decision-Making in Robotics*

MCDM methods have long supported robot selection and evaluation, allowing engineers to compare alternatives across technical and economic criteria [26,27]. One of the most used methods in the field is AHP. The method can be applied when evaluating criteria such as cost, precision, speed, and payload capacity in a hierarchical structure to identify the most suitable system [28]. Another MCDM method used is TOPSIS. The method is implemented in applications such as path planning and material handling, where alternatives are ranked based on their closeness to an ideal solution, considering objectives such as minimizing path length, energy consumption, and obstacle avoidance.

More recent research has shifted to hybrid techniques that combine multiple MCDM methods to leverage their complementary strengths. For example, AHP–TOPSIS frameworks have been proposed for selecting collaborative robots, enabling both weighting and ranking of alternatives [29]. Other hybrid approaches that, for example, integrate fuzzy logic and AI-based models are increasingly adopted to address vagueness and uncertainty in expert judgments. A comprehensive review of advancements in MCDM, highlighting the growing role of hybrid and fuzzy MCDM techniques in robotics, is presented in [30].

## 3. Proposed Multi-Criteria Decision Framework

This chapter presents the proposed MCDM framework for selecting robotic architecture for a 3DCP system. The framework combines AHP and TOPSIS to determine the relative importance of the criteria and then rank the candidate robots. By combining the two methods, it helps decision makers handle uncertainty and subjectivity in the decision process. The evaluation takes into consideration the technical, operational, and economic aspects related to the candidate robots.

### *3.1. Problem Definition*

The proposed MCDM framework helps identify the optimal robotic architecture from a given {A1, A2, A3, A4, . . ., Am} set of candidates (alternatives). Depending on the specifics of the 3DCP application, on-site or off-site, the robot candidates can consist of a large variety of robotic architectures. The candidate's list is the result of a comprehensive review of commercially available and proposed conceptual robotic systems, together with experts' input to ensure the practical feasibility of the candidate systems for the target application.

Besides the robots' candidates list, a set of evaluation criteria $C = \{C_1, C_2, C_3 \ldots C_n\}$ must be defined. The selected criteria are grouped into three main categories: technical, operational, and economic, reflecting the parameters most frequently reported in the literature on robotic systems used in 3D concrete printing applications. Each category contains sub-criteria that detail different aspects relevant to the decision-making process.

Table 1 presents the proposed sub-criteria and provides definitions, indicators, and scoring for each element. The specificity of each criterion is described from the perspective of on-site and off-site applications. For each of the two cases, it is indicated whether the criterion is mandatory or optional. Some of the sub-criteria are application-specific and can be relevant only to certain categories of printed products (e.g., an on-site system that prints buildings in crowded areas). In the analysis process, the designer/engineer team can select which of the optional sub-criteria are relevant or not in the decision process.

**Table 1.** Evaluation criteria for robotic architecture of 3DCP systems.

<table>
<tr><th>Category</th><th>Criteria</th><th colspan="2">Details</th></tr>
<tr><td rowspan="2">C1 Technical</td><td rowspan="2">C1.1 Workspace</td><td colspan="2">Definition: maximum printable space (X × Y × Z) during continuous printing (without repositioning)<br>Indicators: maximum printable volume in $m^3$<br>Scoring: $m^3$ (higher = better)<br>Data source: manufacturer specs, CAD reach maps, kinematic simulation, site measurement</td></tr>
<tr><td>On-site [mandatory criterion]<br>- characterized by large printable volumes<br>- scalable to enable printing of building-scale structures in situ (ex., large horizontal reach and variable height)</td><td>Off-site [mandatory criterion]<br>- the workspace is in relation to the printed object<br>- limited by the available factory cell size or laboratory space<br>- capacity can be expanded through modular cells rather than relying on a single oversized workspace</td></tr>
</table>

**Table 1.** *Cont.*

| Category | Criteria | Details | |
|---|---|---|---|
| C1 Technical | C1.2 Payload capacity | *Definition*: the maximum static and dynamic load the robot can carry<br>*Indicators*: static payload (kg); dynamic payload at printing speed (kg)<br>*Scoring*: kg (*higher = better*)<br>*Data source*: robot's specification sheets, dynamic load testing, finite element analysis for structure/inertia effects | |
| | | *On-site* [mandatory criterion]<br>- extruder plus on-board hopper and additional tooling<br>- must handle varying inertial loads during travel | *Off-site* [mandatory criterion]<br>- payload values could be lower if the material is supplied externally |
| | C1.3 Precision and accuracy | *Definition*: the ability to position the nozzle and deposit material within required tolerances and repeatability over time<br>*Indicators*: repeatability (mm) and absolute positioning accuracy (mm); layer positioning error and nozzle deviation during deposition (mm)<br>*Scoring*: mm (*lower = better*)<br>*Data source*: robot specification sheets, laser tracker measurements, repeatability test runs, printed calibration patterns | |
| | | *On-site* [mandatory criterion]<br>- ground/terrain variability and larger-scale movements may reduce absolute accuracy<br>- robustness to environmental disturbances could be an important factor | *Off-site* [mandatory criterion]<br>- a controlled environment can enable tighter tolerances and higher repeatability |
| | C1.4 Dynamic performance | *Definition*: reflects the ability of the robotic system to position and move the nozzle on predefined trajectories (acceleration/deceleration, max velocity capabilities for a given tool mass) that ensure the required material deposition quality<br>*Note*: the movement speed/acceleration is constrained by the printing process parameters, particularly the rheological properties of the material and the layer deposition requirements. The dynamic performance must ensure sufficient motion smoothness to maintain continuous material flow without deformation and interruption<br>*Indicators*: maximum end effector speed (m/s); maximum acceleration/deceleration (m/s$^2$)<br>*Scoring*: quantitative range-based scoring is applied by comparing each robot's maximum speed $v_i$ and acceleration $a_i$ to a reference range representative of printing-relevant motion conditions ($v_{min},\ v_{max}; a_{min},\ a_{max}$). The normalized sub-scores are computed as shown in Equations (1) and (2): | |
| | | $S_v = \frac{v_i - v_{min}}{v_{max} - v_{min}}$ | (1) |
| | | $S_a = \frac{a_i - a_{min}}{a_{max} - a_{min}}$ | (2) |
| | | The normalized value for the criterion is obtained in Equation (3) by summing the two sub-scores, each multiplied by the weights that reflect their relative importance for the process (e.g., velocity 0.6, acceleration 0.4) | |
| | | $S_{DP} = 0.6S_v + 0.4S_a$ | (3) |
| | | (*higher = better*)<br>*Data source*: manufacturer specs, controller or motion logs, empirical tests | |
| | | *On-site* [mandatory criterion]<br>- slower speeds are often favored in order to ensure build stability and interlayer adhesion | *Off-site* [mandatory criterion]<br>- higher speeds are achievable in off-site facilities, increasing in this way the parts production |

**Table 1.** *Cont.*

<table>
<tr><th>Category</th><th>Criteria</th><th colspan="2">Details</th></tr>
<tr><td rowspan="4">C1 Technical</td><td rowspan="2">C1.5 Ability to Print Complex Geometries</td><td colspan="2">Definition: the ability of the robotic end effector to generate varied trajectories that allow printing of complex geometries<br>Indicators: range of geometries that can be printed: planar and curved (requires 3–4 DoF), non-planar (requires 5–6 DoF), and overhangs (require a minimum of 6 DoF)<br>Scoring: progressive scale based on the complexity of geometries achieved (higher = better)<br>1—basic—planar and curved geometries in a single plane [5]<br>3—intermediate—non-planar printing; trajectories with height variation, gradual slopes [22]<br>5—advanced—ability to print varied complex geometries: complex overhang, multi-directional non-planar paths, lattice structures<br>Note: 2,4—in-between criteria<br>Data source: manufacturer specifications, robot arm kinematics vs. geometry type</td></tr>
<tr><td>On-site [optional criterion]<br>- high adaptability is important because building geometry and constraints can vary widely</td><td>Off-site [optional criterion]<br>- standardized processes minimize the need for extensive variation in printing trajectories for routine parts<br>- if the system is used for building complex architectural components, the robotic system should still be capable of handling specialized trajectories</td></tr>
<tr><td rowspan="2">C1.6 Control complexity</td><td colspan="2">Definition: the level of complexity involved in controlling the robotic system's mechanical structure during 3D concrete printing<br>Note: this criterion becomes especially important when the system is designed or integrated in-house, as it directly impacts development effort, reliability, required expertise, and long-term maintainability<br>Indicators: a complexity index that takes into account the number of axes and DoF; the required sensor suite (e.g., encoders, IMU, vision systems, force-torque sensors, laser scanners); advanced control methods (basic PID, adaptive control, AI-driven control, etc.); and integration effort.<br>Scoring: progressive scale based on the system complexity (lower = better)<br>1 low—Simple gantry system, $\leq$3 DoF, minimal sensors, standard control<br>3 moderate—standard industrial robot arms (e.g., SCARA), 4–6 DoF, basic feedback sensors (e.g., encoders), no advanced control required<br>5 high—multi-axis robotic arm or hybrid system, 6+ DoF, multiple sensors, requires trajectory planning and advanced calibration<br>Note: 2,4—in-between criteria<br>Data source: design reports, academic and industry case studies on similar robotic platforms</td></tr>
<tr><td>On-site [optional criterion]<br>- simpler, more reliable, and easier-to-deploy configurations may be favored<br>- systems should tolerate environmental factors (dust, uneven surfaces, and temperature fluctuations) with minimal calibration needs</td><td>Off-site [optional criterion]<br>- More complex systems can be employed since working conditions are controlled<br>- facilitate the use of more sensors and advanced control methods due to stable conditions and technical support availability</td></tr>
</table>

**Table 1.** *Cont.*

<table>
<tr><th>Category</th><th>Criteria</th><th colspan="2">Details</th></tr>
<tr><td rowspan="6">C2 Operational</td><td rowspan="2">C2.1 Ease of deployment</td><td colspan="2">Definition: Effort and time required to transport, assemble, level, calibrate, and bring the system into operational state on a site/in a factory cell<br>Indicators: number of transportable modules and size/weight per module, setup time (hours), and required crew size, calibration complexity (hours/tests)<br>Scoring: hours, crew numbers (lower setup time and fewer specialists = better)<br>Data source: manufacturer specifications, logistics plans, field deployment reports</td></tr>
<tr><td>On-site [mandatory criterion]<br>- deployment is influenced by transport logistics, site access, and terrain conditions<br>- might require foundation preparation, site leveling, and anchoring to ensure stability<br>- systems that minimize heavy equipment requirements and allow modular setup are generally favored</td><td>Off-site [mandatory criterion]<br>- deployment is usually simpler due to the controlled environment (factory floor, fixed utilities)</td></tr>
<tr><td rowspan="2">C2.2 Automation Level</td><td colspan="2">Definition: the capability of the robotic system to operate independently, versus requiring human intervention<br>Indicators: progressive scale based on degree of autonomy: manual operation, semi-automated functions, or fully autonomous task execution<br>Scoring: progressive scale (higher = better)<br>1—moderate automation—range from manual/operator-driven automation to semi-automated functioning (predefined toolpaths, automatic start/stop); human intervention required for setup, supervision, and error recovery<br>3—high automation—autonomous printing operations with real-time monitoring and error detection; human role limited to supervision and material supply<br>5—full automation—fully autonomous operation, including calibration, monitoring, error correction, and shutdown; human role reduced to oversight and emergency handling<br>Note: 2,4—in between criteria<br>Data source: design reports, technical documentation, academic and industry case studies</td></tr>
<tr><td>On-site [optional criterion]<br>- higher autonomy reduces labor requirements and operator risks in challenging or hazardous construction environments<br>- unpredictable conditions (weather, terrain variability, material inconsistencies) may limit full autonomy</td><td>Off-site [optional criterion]<br>- controlled environments make higher levels of automation more feasible<br>- can significantly reduce manpower needs and improve repeatability and throughput</td></tr>
<tr><td rowspan="2">C2.3 Compatibility with site space constraints</td><td colspan="2">Definition: the degree to which the robot architecture adapts to or fits within constrained environments (e.g., a site or factory cell) or irregular terrain in on-site applications<br>Indicators: footprint dimensions when deployed ($m^2$), minimum overhead clearance required (m)<br>Scoring: $m^2$, m (lower footprint and clearance required = better for constrained sites)<br>Data source: site layout analysis</td></tr>
<tr><td>On-site [mandatory criterion]<br>- tight urban sites, limited crane access, and overhead obstructions require compact or modular systems</td><td>Off-site [optional criterion]<br>- less constraint, but factory cell size and material provider subsystems still introduce constraints</td></tr>
</table>

**Table 1.** *Cont.*

| Category | Criteria | Details | |
|---|---|---|---|
| C2 Operational | C2.4 Operational flexibility | *Definition*: the ability to easily reposition and extend printing coverage during ongoing operations without complex reconfiguration<br>*Indicators*: presence of wheels/tracks<br>*Scoring*: ordinal scale from 1 to 5, where 1 = no mobility; 3 = limited repositioning; 5 = self-propelled (higher value = better)<br>*Data source*: manufacturer specification, field test/reports | |
| | | *On-site* [optional criterion]<br>- important for printing large structures | *Off-site* [optional criterion]<br>- not that relevant; it could be useful in case of factory cell reconfiguration |
| | C2.5 Operational environment resistance | *Definition*: robustness to dust, humidity, temperature variations, vibration, and weather<br>*Indicators*: Ingress Protection (IP) rating, Operating temperature/humidity range, Vibration tolerance, and shock rating<br>*Scoring*: IP level, °C/% (*higher resistance = better for on-site*)<br>*Data source*: environmental test reports, certification paperwork | |
| | | *On-site* [mandatory criterion]<br>- environmental resistance is very important, and it strongly influences system reliability and safety | *Off-site* [optional criterion]<br>- environmental resistance is less critical because the controlled environment minimizes exposure to dust, moisture, temperature fluctuations, and weather |
| | C2.6 Functional Extensibility | *Definition*: the ability of the robotic system to be upgraded or reconfigured for additional processes: reinforcement placement, multi-material nozzles, finishing tools<br>*Indicators*: hardware compatibility for modular tools, software adaptability for new process modules, capacity to integrate multiple tasks within a workflow<br>*Scoring*: progressive scale (*higher = better*)<br>*1 low*—rigid architecture; no possibility of adding new tools or processes<br>*3 moderate*—some modularity available; can add certain tools (e.g., finishing nozzle) with moderate integration effort<br>*5 high*—supports multiple extensions with minor adjustments<br>Note: 2,4—in between criteria<br>*Data source*: technical documentation, case studies, design documents | |
| | | *On-site* [optional criterion]<br>- integrating reinforcement/finishing tools during printing could be desirable and could avoid manual post-processing<br>- multi-material nozzles could be useful for adding insulation, adhesives, or sealants directly during construction, but it might be logistically challenging to implement | *Off-site* [optional criterion]<br>- reinforcements placement by system is not essential since factory setups allow for easy conventional reinforcement insertion<br>- controlled conditions favor multi-material nozzles and allow implementation of advanced multi-material applications<br>- finishing tools are less desirable; finishing can be carried out easily after printing, using conventional approaches |

**Table 1.** *Cont.*

<table>
<tr><th>Category</th><th>Criteria</th><th colspan="2">Details</th></tr>
<tr><td rowspan="6">C3 Economic</td><td rowspan="2">C3.1<br>Capital cost</td><td colspan="2">Definition: initial expenditure needed to purchase/manufacture and deploy the robotic system before the first print<br>Indicators: acquisition price of the robotic system, logistics, and on-site building costs<br>Scoring: total initial cost (lower = better)<br>Data source: vendor quotes, site preparation cost estimates</td></tr>
<tr><td>On-site [optional criterion]<br>- the large dimensions of printed elements may require greater system size and adaptability, leading to higher initial costs<br>- the robotic system should be modular to allow transport, setup, and dismantling on different sites, which can further increase initial costs</td><td>Off-site [optional criterion]<br>- prefabricated elements are usually smaller than those printed on-site, which reduces the required size of the robotic structure and lowers initial cost<br>- because the system remains in a fixed location, modularity for frequent relocation is unnecessary, reducing capital costs compared to on-site deployment</td></tr>
<tr><td rowspan="2">C3.2<br>Operational costs</td><td colspan="2">Definition: costs needed to operate the system: energy consumption, consumables, and operator labor<br>Indicators: energy demand per volume of material deposited, consumables usage and replacement frequency, operator labor hours required for setup, supervision, and error handling<br>Scoring:<br>1 Very Low—energy-efficient system; minimal consumables; low labor demand due to automation<br>3 Moderate—manageable energy and labor requirements; consumables replaced periodically<br>5 Very High—high energy consumption; many consumables; high labor dependency.<br>Note: 2,4—in between criteria<br>Data source: vendor specifications, project case studies, and cost reports</td></tr>
<tr><td>On-site [optional criterion]<br>- relevant criterion due to operational costs, which are typically higher due to frequent calibration, environmental protection needs, and increased risk of errors</td><td>Off-site [optional criterion]<br>- operational costs are generally lower</td></tr>
<tr><td rowspan="2">C3.3<br>Maintenance cost</td><td colspan="2">Definition: costs and downtime associated with regular servicing, spare parts, repairs, cleaning, and preventive maintenance.<br>Indicators: annual spare parts cost, annual downtime cost<br>Scoring: annual total maintenance cost (lower = better)<br>Data source: vendor maintenance and servicing manual, maintenance logs from similar machines, case studies</td></tr>
<tr><td>On-site [optional criterion]<br>- the working environment has a more negative effect on the system and may increase maintenance<br>- the maintenance cost could have an important impact on profitability margins</td><td>Off-site [optional criterion]<br>- controlled environment reduces failure rate and service complexity</td></tr>
</table>

The above criteria contain both quantitative and qualitative indicators. The quantitative criteria, such as payload capacity, workspace dimensions, end-effector velocity, and deposition accuracy, are derived from manufacturer datasheets, experimental measurements, or simulation results. Qualitative criteria, including adaptability, ease of deployment, and environmental resistance, are assessed using expert judgment, literature surveys, or structured scoring scales.

*3.2. Multi-Criteria Decision-Making Procedure*

The proposed framework contains five steps. Next, each of these steps is described, emphasizing the input data and obtained outputs/results in each phase.

***Step 1****—Problem structuring*

The decision goal in this case is the selection of an optimal robotic architecture for a 3DCP system. At this stage, the specific applications of the designed system must be defined. The evaluation criteria presented in the previous subsection are analyzed, and the applicable ones for the application are selected (*n—number of criteria*).

- *Input(s)*: goal of the selection process
- *Output(s)*: characteristics of the process, environment, and printed products; criteria used in the decision process

***Step 2****—Criteria weighting with AHP*

Next, the relative weights of each criterion in relation to the 3DCP system application are determined. For this purpose, the pairwise comparison matrix $A$ is created using the Saaty fundamental scale. At this stage, each criterion is compared with every other criterion in its group according to scale. The scale uses integer numbers, where 1 indicates equal importance, 3 moderate importance, 5 strong importance, 7 very strong importance, 9 extreme importance, and 2, 4, 6, and 8 represent intermediate values between these judgments. The entries of the comparison matrix are obtained from experts' evaluation. The general form of the comparison matrices is

$$A = \begin{bmatrix} 1 & a_{12} & a_{13} & \dots & a_{1n} \\ \frac{1}{a_{12}} & 1 & a_{21} & \dots & a_{2n} \\ \frac{1}{a_{13}} & \frac{1}{a_{23}} & 1 & \dots & a_{3n} \\ \dots & \dots & \dots & \dots & \dots \\ \frac{1}{a_{1n}} & \frac{1}{a_{2n}} & \frac{1}{a_{3n}} & \dots & 1 \end{bmatrix} \quad (4)$$

where: $a_{ij} > 0$ and $a_{ji} = 1/a_{ij}$, $\{i = 1,\dots,n;\ j = 1,\dots,n\}$

Using the matrix $A$, the priority vector (weights) $\omega$ is calculated. All alternatives are assumed to have equal importance, and weighting is applied only at the criterion level using the AHP-derived priority vector. The vector $\omega$ assigns a weight to each selected criterion.

$$\omega = (\omega_1, \omega_2, \omega_3,\ \dots,\ \omega_n)^T \quad (5)$$

To obtain $\omega$, Equation (6) is used:

$$A\omega = \lambda_{max}\omega \quad (6)$$

where: $\lambda_{max}$ represents the maximum eigenvalue of the matrix $A$.

To ensure the reliability of the pairwise comparison matrix, both Consistency Index ($CI$) and Consistency Ratio ($CR$) values must be determined:

$$CI = \frac{\lambda_{max} - n}{n - 1} \quad (7)$$

$$CR = \frac{CI}{RI} \quad (8)$$

where: $RI$ is the Random Index corresponding to the matrix order $n$.

The value of the $CR$ should be less than 0.1 to ensure acceptable consistency of judgments. If the values are higher, the pairwise comparisons must be revised.

- *Input(s)*: criteria used in the decision process, relative importance of each criterion in relation to the designed systems
- *Output(s)*: Comparison matrix $A$, priority vector $\omega$

***Step 3***—*Construction of the Decision Matrix*

Once the weights are established, TOPSIS is applied to rank the candidate robotic systems. This method evaluates each candidate robotic system based on its closeness to an ideal solution (best possible performance across all criteria) and its distance from a negative-ideal solution (worst performance).

The process starts by constructing the decision matrix $D$:

$$D = \begin{bmatrix} x_{11} & x_{12} & \dots & x_{1n} \\ x_{21} & x_{22} & \dots & x_{2n} \\ \dots & \dots & \dots & \dots \\ x_{m1} & x_{m2} & \dots & x_{mn} \end{bmatrix} \tag{9}$$

The decision matrix $D$ integrates both quantitative and qualitative criteria. The qualitative attributes are represented by numerical scores derived from predefined linguistic scales as introduced in Section 3.1 when the criteria were defined.

- *Input(s)*: candidate robotic architectures (alternatives), evaluation criteria, and scoring scales
- *Output(s)*: decision matrix $D$

***Step 4***—*Application of TOPSIS*

The matrix $D$ is normalized using vector normalization. For each criterion $j \in \{1,\ldots,n\}$ the Euclidean norm is computed:

$$\|x_j\| = \sqrt{\sum_{i=1}^{m} x_{ij}^2} \tag{10}$$

The normalized decision matrix $R = [r_{ij}]$ is obtained using:

$$r_{ij} = \frac{x_{ij}}{\|x_j\|} \qquad i = 1, \ldots, m, \quad j = 1, \ldots, n \tag{11}$$

The normalized matrix $R$ is multiplied with the criteria weight vector $\omega$ to form the weighted normalized decision matrix $V$:

$$V = [v_{ij}]_{mxn} \quad \text{where}: \; v_{ij} = \omega_j r_{ij} \tag{12}$$

From $V$, the positive ideal and negative ideal solutions are determined depending on the criterion type. For benefit criteria:

$$v_j^+ = \max_i(v_{ij}), \qquad v_j^- = \min_i(v_{ij}) \tag{13}$$

For cost criteria:

$$v_j^+ = \min_i(v_{ij}), \qquad v_j^- = \max_i(v_{ij}) \tag{14}$$

Next, the Euclidean distance of each alternative from the ideal and negative-ideal solutions is calculated:

$$S_i^+ = \sqrt{\sum_{j=1}^{n}\left(v_{ij} - v_j^+\right)^2} \qquad S_i^- = \sqrt{\sum_{j=1}^{n}\left(v_{ij} - v_j^-\right)^2} \tag{15}$$

- *Input(s)*: Priority vector $\omega$, decision matrix $D$, criteria type information (benefit/cost)
- *Output(s)*: Euclidean distances for each alternative $S_i^+$, $S_i^-$

***Step 5**—Ranking of Alternatives*

At this step, the closeness coefficient is obtained:

$$CC_i = \frac{S_i^-}{S_i^+ + S_i^-}, \qquad 0 \le CC_i \le 1 \tag{16}$$

The alternatives are ranked based on $CC_i$, with higher values indicating closer proximity to the ideal solution.

- *Input(s)*: Euclidean distances for each alternative $S_i^+$, $S_i^-$
- *Output(s)*: optimal solution for the given application.

## 4. MCDM Case Study of a 3DCP System for Off-Site Façade Printing

To test the proposed selection MCDM framework, a case study was developed. In this case study, a laboratory-scale 3DCP system intended for printing façade elements is analyzed. The primary objectives for the system are the production of high-quality demonstrators and research flexibility rather than mass production. Three robot architectures ($m$ = 3) were evaluated for this purpose: a gantry robot (A1) (Figure 4a), a Kuka robot arm (A2) with 6 DoF (Figure 4b), and a parallel Delta robot (A3) (Figure 4c).

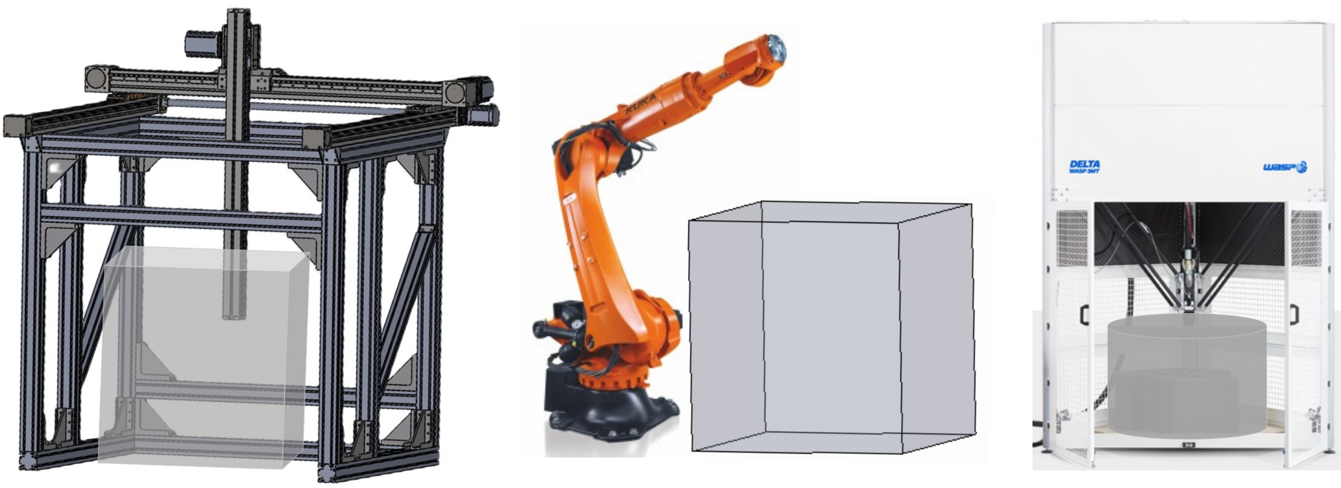

(**a**) (**b**) (**c**)

**Figure 4.** Proposed robot architectures (**a**) gantry robot, (**b**) Kuka robot arm, (**c**) delta robot.

To implement the proposed MCDM framework, a multidisciplinary expert panel was formed, consisting of one university professor in mechatronics engineering and one MSc-qualified mechatronics engineer with professional experience in robotics, as well as two university professors in civil engineering with expertise in concrete materials and structural behavior. The robotics experts focused on aspects related to robot design and performance, such as kinematics, control complexity, and dynamic behavior, while the civil engineers contributed expertise on construction constraints, material deposition, operational feasibility, and cost considerations in 3DCP. The team's tasks included selecting the relevant evaluation criteria for the façade printing application, collecting and validating the quantitative and qualitative parameters for the three candidate robots, performing the AHP-TOPSIS analysis, and critically interpreting the resulting rankings.

The gantry robot is an in-house design proposal. The parameters used in the analysis were extracted from the design documentation, component datasheets, and expert input. The system has three DoF, with overall dimensions of 2.1 × 2 × 1.8 m (L × W × H), and a payload capacity of 35 kg. The workspace of the robot is 0.9 $m^3$, and its end effector can be positioned with a precision of 2.5 mm. The linear actuators used have a maximum velocity of 0.1 m/s and a maximum acceleration of 0.5 $m/s^2$.

The robot arm is produced by Kuka (Germany, Augsburg), model KR 120 R2700-2 with 6 DoF. Parameter values were taken from the manufacturer's technical documentation and datasheets and refined through expert input. For comparability across alternatives, a 1.1 $m^3$ effective printing volume within the robot's reachable workspace was selected. The rated payload of the robot is 120 kg with a repeatability of ±0.05 mm. For this application, a maximum positioning precision of 1 mm was considered (even though the robot's precision is better than 1 mm). The high-velocity servos of the robot allow the end-effector to obtain, in ideal conditions, high maximum speeds. For this application, an average of 1 m/s is considered and an acceleration of a maximum of 2 $m/s^2$.

The Delta robot is produced by WASP (Italy, Massa Lombarda) and is commercialized as a part of the 3DCP printer model 3MT. Parameter values were based on manufacturer documentation, datasheets, the producer's website, and experts' inputs. The robotic systems have 3 DoF. The overall dimension of the system is 2.15 × 2.35 × 3.05 m (L × W × H) with a cylindrical workspace of 0.785 $m^3$. The delta robot has a 45 kg payload and a precision of 2 mm. Based on the manufacturer's datasheet, the velocity of the end effector during printing/free movement can reach a maximum of 0.2 m/s and a maximum acceleration of 0.15 $m/s^2$.

The values for the criteria related to deployment time, operational cost, and maintenance cost were estimated by the expert team. The capital cost for each alternative was obtained from the manufacturers' official websites for A2 and A3 and from the design bill of materials (BOM) for the gantry system (A1).

As a first step, the relevant sub-criteria defined in Chapter 3 are selected. For this application the following $n$ = 12 sub-criteria were selected {C1.1—workspace; C1.2—payload; C1.3—precision; C1.4—dynamic performance; C1.5—print complex geometries; C1.6—control complexity; C2.1—ease of deployment; C2.2—automation level; C2.3—compatibility with site space constraints; C3.1—capital cost; C3.2—operational cost; C3.3—maintenance cost}.

Next, the weights were assigned to each selected sub-criterion by constructing the comparison matrix $A$. The pairwise comparisons were provided by the expert team. The experts first gave their assessments independently using the Saaty scale, after which the results were discussed and combined to reach a common evaluation. For example, precision C1.3 was judged to be moderately more important than workspace C1.1, leading to a Saaty value of 1/2, while printing complex geometries C1.5 was considered strongly more important than ease of deployment C2.1, resulting in a value of 4. The consistency of the resulting comparison matrix was then checked using the AHP consistency indices ($CI$ and $CR$). Table 2 presents the corresponding Saaty scale scores for each selected sub-criterion.

**Table 2.** Developed comparison matrix *A*.

| *Criteria* | C1.1 | C1.2 | C1.3 | C1.4 | C1.5 | C1.6 | C2.1 | C2.2 | C2.3 | C3.1 | C3.2 | C3.3 |
|---|---|---|---|---|---|---|---|---|---|---|---|---|
| **C1.1** | 1 | 2 | 1/2 | 3 | 1/2 | 3 | 5 | 4 | 4 | 1 | 5 | 4 |
| **C1.2** | 1/2 | 1 | 1/3 | 2 | 1/2 | 3 | 4 | 3 | 3 | 2 | 3 | 4 |
| **C1.3** | 2 | 3 | 1 | 2 | 1 | 3 | 3 | 5 | 4 | 3 | 3 | 4 |
| **C1.4** | 1/3 | 1/2 | 1/2 | 1 | 1/3 | 2 | 4 | 2 | 4 | 1/3 | 3 | 3 |
| **C1.5** | 2 | 2 | 1 | 3 | 1 | 4 | 4 | 4 | 5 | 2 | 4 | 4 |
| **C1.6** | 1/3 | 1/3 | 1/3 | 1/2 | 1/4 | 1 | 3 | 2 | 1 | 1/3 | 3 | 2 |
| **C2.1** | 1/5 | 1/4 | 1/3 | 1/4 | 1/4 | 1/3 | 1 | 1/3 | 2 | 1/5 | 1/2 | 1/2 |
| **C2.2** | 1/4 | 1/3 | 1/5 | 1/2 | 1/4 | 1/2 | 3 | 1 | 3 | 1/2 | 2 | 2 |
| **C2.3** | 1/4 | 1/3 | 1/4 | 1/4 | 1/5 | 1/4 | 1/2 | 1/3 | 1 | 1/3 | 1/2 | 1/2 |
| **C3.1** | 1 | 1/2 | 1/3 | 3 | 1/2 | 3 | 5 | 2 | 3 | 1 | 4 | 2 |
| **C3.2** | 1/5 | 1/3 | 1/3 | 1/3 | 1/4 | 1/3 | 2 | 1/2 | 2 | 1/4 | 1 | 1 |
| **C3.3** | 1/4 | 1/4 | 1/4 | 1/3 | 1/4 | 1/2 | 2 | 1/2 | 2 | 1/2 | 1 | 1 |

The obtained priority vector $\omega$ presented in Figure 5 reflects the requirements of the laboratory-scale façade 3D concrete printing application. Precision C1.3 and the ability to print complex geometries C1.5 emerge as the most influential criteria, with weights of 0.1750 and 0.1716, respectively, emphasizing the importance of dimensional accuracy and flexible end-effector trajectory generation. Workspace C1.1 and payload C1.2 are next in importance, supporting the printing of large façade elements while maintaining system stability. Capital cost C3.1 also remains relevant, reflecting the need to consider initial investment constraints. Criteria related to operational performance, usability, and operational costs exhibit lower influence, which is consistent with a research-oriented laboratory context.

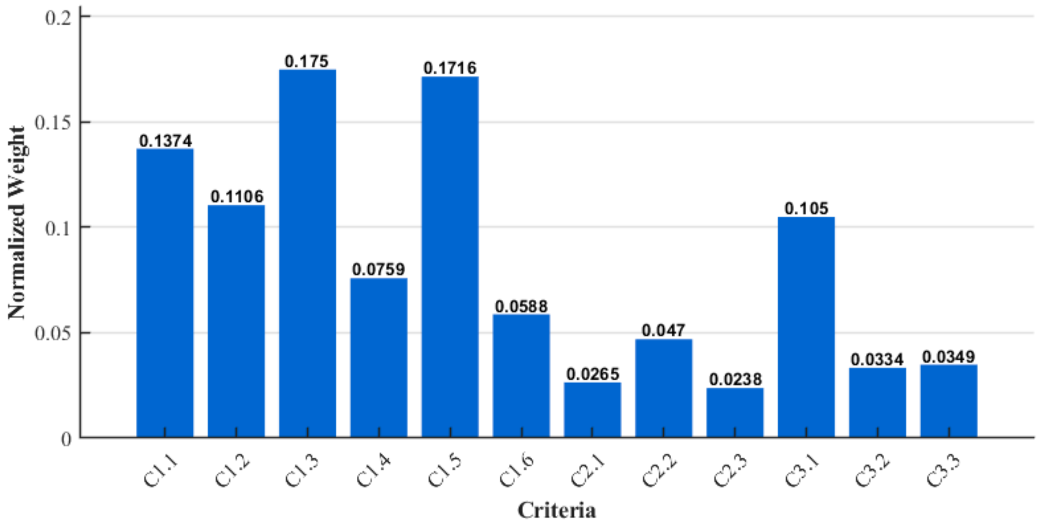


**Figure 5.** Normalized AHP weight distribution.

The maximum eigenvalue $\lambda_{max}$ for the comparison matrix, *A* was 12.8329. This value was used in Equation (7) to calculate the *CI* index, resulting in a value of 0.0757. The *RI* used for the calculation of the *CR* was 1.54, corresponding to a $12 \times 12$ comparison matrix. Using Equation (8), the *CR* was calculated as 0.0492, indicating an acceptable level of consistency, since the obtained value is below the recommended limit of 0.1.

Next, the decision matrix *D* is built. For this, scores are assigned to the three alternatives, A1, A2, and A3, on each criterion. The values are provided as described in Section 3.1, under the “Indicators” and “Scoring” subsections for each criterion. Each criterion is also classified as either a benefit (higher values are better) or a cost (lower values are better). The resulting data for the current case study are summarized in Table 3.

**Table 3.** AHP decision criteria.

| Criteria *Cx.y* | Description | Weight $\omega$ | Gantry System (A1) | Robotic Arm (A2) | Delta Robot (A3) |
|---|---|---|---|---|---|
| C1.1 | Workspace [$m^3$] (*higher better*) | 0.1374 | 0.9 | 1.1 | 0.785 |
| C1.2 | Payload [kg] (*higher better*) | 0.1106 | 35 | 120 | 45 |
| C1.3 | Precision [mm] (*lower values better*) | 0.1750 | 2.5 | 1 | 2 |
| C1.4 | Dynamic performance (*higher better*) | 0.0759 | 0.110 | 0.862 | 0.334 |
| C1.5 | Print complex geometries (1–5 scale) (*higher better*) | 0.1716 | 1 | 3 | 1 |
| C1.6 | Control complexity (*lower better*) | 0.0588 | 1 | 3 | 3 |
| C2.1 | Ease of deployment [hours] (*lower better*) | 0.0265 | 24 | 32 | 16 |
| C2.2 | Automation level (1–5 scale) (*higher better*) | 0.0470 | 1 | 2 | 3 |
| C2.3 | Compatibility with site space constraints [$m^2$] (*lower better*) | 0.0238 | 4.2 | 6 | 5.05 |
| C3.1 | Capital cost [€](*lower better*) | 0.1050 | 25,000 | 100,000 | 60,335 |
| C3.2 | Operational cost (1–5 scale) (*lower better*) | 0.0334 | 2 | 3 | 2 |
| C3.3 | Maintenance cost [€/year] (*lower better*) | 0.0349 | 1800 | 5500 | 3000 |

The values from matrix $D$ are used to calculate the normalized decision matrix $R$. The normalized components $r_{ij}$ are obtained by applying Equation (11), in which each element $x_{ij}$ is divided by the Euclidean norm of its corresponding criterion, calculated according to Equation (10). The normalized matrix $R$ is then weighed using the priority vector $\omega$, resulting in the weighted normalized decision matrix $V$.

The normalized decision matrix $V$ is used to determine the positive ideal and negative ideal solutions for each criterion, taking into account criterion type (benefit/cost). Table 4 presents the ideal and negative-ideal values obtained for each criterion.

**Table 4.** Positive ideal and negative ideal values for each criterion.

| Criterion | Type | Ideal Solution | Negative Ideal Solution |
|---|---|---|---|
| C1.1 | Benefit | 0.09310 | 0.06644 |
| C1.2 | Benefit | 0.09994 | 0.02915 |
| C1.3 | Cost | 0.09998 | 0.13046 |
| C1.4 | Benefit | 0.07030 | 0.00897 |
| C1.5 | Benefit | 0.15520 | 0.05173 |
| C1.6 | Cost | 0.01348 | 0.04045 |
| C2.1 | Cost | 0.00983 | 0.01966 |
| C2.2 | Benefit | 0.03770 | 0.01256 |
| C2.3 | Cost | 0.01121 | 0.01602 |
| C3.1 | Cost | 0.02197 | 0.08790 |
| C3.2 | Cost | 0.01621 | 0.02432 |
| C3.3 | Cost | 0.00964 | 0.02946 |

The ideal and negative ideal solutions are used to calculate the Euclidean distance of each alternative. Further, the closeness coefficient $CC_i$ is calculated using Equation (16). The obtained data are presented in Table 5.

**Table 5.** TOPSIS evaluation—ranking of the candidate robots.

| Alternative | S+ (to Ideal Best) | S− (to Ideal Worst) | Closeness Coefficient $CC_i$ |
|---|---|---|---|
| A1—Gantry System | 0.1629 | 0.0753 | 0.3162 |
| A2—Robotic Arm | 0.0762 | 0.1627 | 0.6810 |
| A3—Delta Robot | 0.1471 | 0.0573 | 0.2802 |

The obtained results after implementing TOPSIS are presented in Figure 6. It can be observed that the robotic arm A2 obtained the highest closeness coefficient, $CC_2 = 0.6810$, indicating the best overall performance among the evaluated alternatives. The result is primarily driven by the robotic arm's superior performance in key quantitative criteria, including higher payload capacity, improved positioning precision, and enhanced dynamic performance, which are essential for façade 3D concrete printing applications. In particular, the robotic arm offers significantly higher payload capacity and precision compared to the gantry (A1) and delta (A3) systems, as well as greater flexibility in executing complex printing trajectories. The gantry system (A1) and delta robot (A3) exhibit lower and comparable performance levels ($CC_1 = 0.3162$ and $CC_3 = 0.2802$, respectively), reflecting more limited capabilities in these dominant criteria.

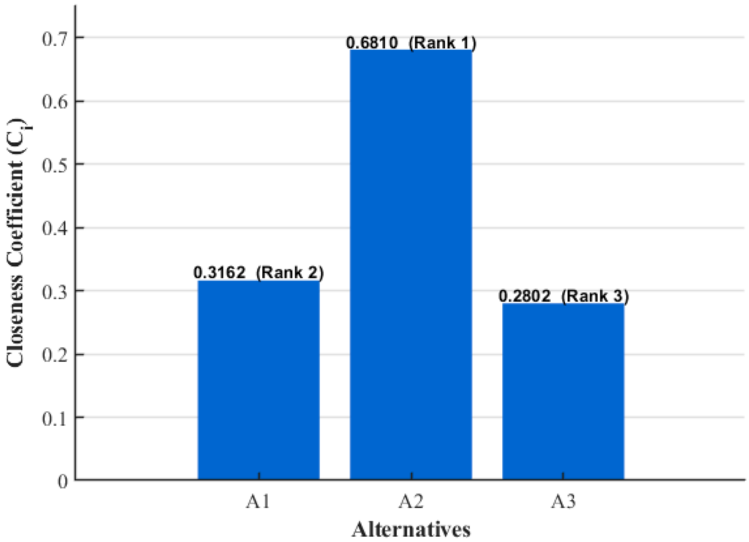


**Figure 6.** TOPSIS Ranking of Alternatives.

To assess the robustness of the proposed AHP–TOPSIS decision framework, a sensitivity analysis was performed by varying the weights of the three highest-ranked criteria: precision C1.3, the ability to print complex geometries C1.5, and workspace C1.1. Each criterion weight was independently modified by ±10% and ±20%, and after each change, the full weight vector was renormalized, and the TOPSIS method was applied again. Figure 7 shows the variation of the TOPSIS closeness coefficients for the three alternatives (A1, A2, and A3) under each perturbation scenario. While changes in the weights lead to gradual and monotonic variations in the closeness coefficients, particularly for workspace and complex geometry capability, no ranking reversals are observed across any scenario. This indicates that the final ranking remains stable and that the proposed MCDM framework is robust to reasonable changes in the most influential criteria.

The results of the case study indicate that the robotic arm (A2) is the most suitable architecture for the considered off-site façade 3D concrete printing application. This finding is consistent with previous 3DCP studies, which report that multi-axis articulated robots can follow complex, non-planar paths and provide improved control of nozzle orientation compared to gantry and parallel systems. These capabilities support the fabrication of geometrically complex components with higher surface quality and dimensional accuracy, which are important requirements in façade applications [22,31]. Also, several façade-oriented 3DCP studies [31,32] highlight that articulated robotic arms are well suited to controlled, off-site environments, where precision, payload handling, and trajectory flexibility are more influential than, for example, deployment time and site space constraints. These characteristics align with the dominant criteria identified by the AHP weighting process in this study, namely precision, ability to print complex geometries, and dynamic performance.

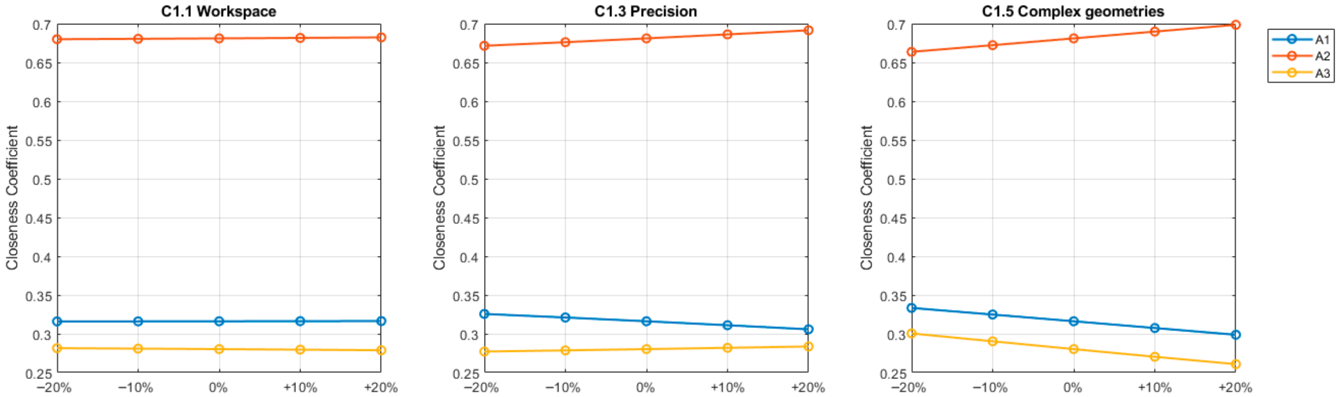


**Figure 7.** Sensitivity analysis of TOPSIS results under-weight variations.

While the results are promising, several limitations of the present case study should be noted. First, the analysis considered only three representative robotic architectures and did not include emerging hybrid, mobile, or cable-driven systems that may offer alternative performance characteristics. Second, the selection of criteria and their associated weights was based on expert judgment and may vary depending on specific project goals, practical constraints, or stakeholder priorities. For example, the case study does not explicitly evaluate the suitability of the robotic systems for integrated reinforcement strategies. This reflects the laboratory-scale, demonstrator-oriented scope of the application, where structural reinforcement was not required. However, the proposed MCDM framework is designed to accommodate such aspects through the C2.6 Functional Extensibility criterion. Although this criterion was not applied in the present analysis, it can be incorporated in future studies addressing structurally reinforced 3D concrete printing applications. Third, several criterion values were derived from manufacturer datasheets and expert estimations rather than experimental validation under operational printing conditions. As a result, for some parameters, the actual performance may differ slightly from the assumed values.

## 5. Conclusions

This study proposed an MCDM framework for the systematic selection of robotic architecture for 3DCP applications. The integration of AHP and TOPSIS allows a structured and quantitative evaluation of technical, operational, and economic trade-offs. This approach reduces reliance on purely subjective assessments. The framework is structured around 15 decision criteria, grouped into three main categories and supported by a transparent step-by-step implementation procedure, facilitating its application in different 3DCP contexts.

The applicability of the framework was demonstrated through a case study focused on a laboratory-scale, off-site 3DCP system for façade element fabrication. Three representative robotic configurations were analyzed: a gantry system, an articulated robot arm, and a delta robot. The results show that the articulated robotic arm achieved the highest TOPSIS closeness coefficient ($CC_2$ = 0.6810), indicating the best overall performance among the considered alternatives. This outcome is primarily attributed to its ability to follow complex, non-planar trajectories, provide improved control of nozzle orientation, and maintain high geometric accuracy. These characteristics are important requirements for façade-oriented 3DCP applications. The obtained results are consistent with recent literature on robotic concrete printing and confirm the effectiveness of the proposed framework in supporting application-driven robot selection.

Despite these promising results, several limitations of the present study were highlighted. The analysis was restricted to three representative robotic architectures, relied on expert judgment for criteria selection and weighting, and used manufacturer datasheets and expert estimations rather than experimental validation, which may lead to differences between assumed and actual performance.

Future work will address these limitations by applying the proposed framework to a broader range of 3DCP applications. The analysis will be extended to additional robotic configurations and supported by experimental performance data. Moreover, the integration of fuzzy or hybrid fuzzy–AHP/TOPSIS approaches is planned to better capture uncertainty in expert judgments. Overall, the proposed framework provides a flexible and robust decision-support tool for informed early-stage selection and design of robotic systems for diverse 3D concrete printing applications.

**Author Contributions:** Conceptualization, C.L., C.M.N. and I.S.; methodology, C.L., C.M.N. and I.S.; software, C.L.; validation, C.L., C.M.N. and I.S.; formal analysis, C.L., C.M.N. and I.S.; investigation, C.L. and I.S.; resources, I.S.; data curation, C.L.; writing—original draft preparation, C.L., C.M.N. and I.S.; writing—review and editing, C.L., C.M.N. and I.S.; visualization, C.L., C.M.N. and I.S.; supervision, C.L. and I.S.; project administration, I.S.; funding acquisition, I.S. All authors have read and agreed to the published version of the manuscript.

**Funding:** This work was supported by a grant from the Ministry of Research, Innovation, and Digitization, CCCDI—UEFISCDI, project number PN-IV-P7-7.1-PED-2024-2692, within PNCDI IV.

**Data Availability Statement:** The original contributions presented in this study are included in the article. Further inquiries can be directed to the corresponding author.

**Acknowledgments:** The authors express their thanks for the support offered by the Intelligent Mechatronic Systems Laboratory (IMSLab) at the Technical University of Cluj-Napoca in developing the research presented in the paper.

**Conflicts of Interest:** The authors declare no conflicts of interest.

## Abbreviations

The following abbreviations are used in this manuscript:

| | |
|---|---|
| 3DCP | 3D Concrete Printing |
| AHP | Analytic Hierarchy Process |
| TOPSIS | Technique for Order Preference by Similarity to Ideal Solution |
| MCDM | Multi-Criteria Decision-Making |
| DoF | Degrees of Freedom |
| IP | Ingress Protection |
| *CI* | Consistency Index |
| *CR* | Consistency Ratio |
| *RI* | Random Index |

## References

1. Luo, F.; Li, R.Y.M.; Crabbe, M.J.C.; Pu, R. Economic development and construction safety research: A bibliometrics approach. *Saf. Sci.* **2022**, *145*, 105519. [CrossRef]
2. United Nations Environment Programme. *Global Status Report for Buildings and Construction: Towards a Zero-Emission, Efficient and Resilient Buildings and Construction Sector*; UNEP: Nairobi, Kenya, 2023; Available online: https://digitallibrary.un.org/record/3995803?ln=en&v=pdf (accessed on 9 December 2025).
3. Juricic, B.B.; Galic, M.; Marenjak, S. Review of the Construction Labour Demand and Shortages in the EU. *Buildings* **2021**, *11*, 17. [CrossRef]
4. Tu, H.; Wei, Z.; Bahrami, A.; Kahla, N.B.; Ahmad, A.; Özkılıç, Y.O. Recent advancements and future trends in 3D concrete printing using waste materials. *Dev. Built Environ.* **2023**, *16*, 100187. [CrossRef]

5. Singh, N.; Colangelo, F.; Farina, I. Sustainable non-conventional concrete 3D printing—A review. *Sustainability* **2023**, *15*, 10121. [CrossRef]
6. Girskas, G.; Kligys, M. 3D Concrete Printing Review: Equipment, Materials, Mix Design, and Properties. *Buildings* **2025**, *15*, 2049. [CrossRef]
7. Bekkering, J.; Kuit, B.; Biffi, A.; Ahmed, Z.Y. Architectonic explorations of the possibilities of 3D concrete printing: The historic building fragment as inspiration for new applications with 3D concrete printing in architecture. In *RILEM International Conference on Concrete and Digital Fabrication*; Springer: Berlin/Heidelberg, Germany, 2020; pp. 1078–1090. [CrossRef]
8. Mohammad, M.; Masad, E.; Al-Ghamdi, S.G. 3D concrete printing sustainability: A comparative life cycle assessment of four construction method scenarios. *Buildings* **2020**, *10*, 245. [CrossRef]
9. Alhumayani, H.; Gomaa, M.; Soebarto, V.; Jabi, W. Environmental assessment of large-scale 3D printing in construction: A comparative study between cob and concrete. *J. Clean. Prod.* **2020**, *270*, 122463. [CrossRef]
10. Bhattacherjee, S.; Basavaraj, A.S.; Rahul, A.V.; Santhanam, M.; Gettu, R.; Panda, B.; Mechtcherine, V. Sustainable materials for 3D concrete printing. *Cem. Concr. Compos.* **2021**, *122*, 104156. [CrossRef]
11. Batikha, M.; Jotangia, R.; Baaj, M.Y.; Mousleh, I. 3D concrete printing for sustainable and economical construction: A comparative study. *Autom. Constr.* **2022**, *134*, 104087. [CrossRef]
12. Albalkhy, W.; Valera, E.H.; Karmaoui, D.; Lafhaj, Z.; Linner, T.; Ayadi, S.; Boutabba, A. Motives and Barriers for Offsite and Onsite Construction 3D Printing. In Proceedings of the International Symposium on Automation and Robotics in Construction (ISARC), Lille, France, 3–5 June 2024; Volume 41, pp. 1190–1197. [CrossRef]
13. Xu, W.; Huang, S.; Han, D.; Zhang, Z.; Gao, Y.; Feng, P.; Zhang, D. Toward automated construction: The design-to-printing workflow for a robotic in-situ 3D printed house. *Case Stud. Constr. Mater.* **2022**, *17*, e01442. [CrossRef]
14. Zuo, Z.; Zhang, Y.; Li, J.; Huang, Y.; Zhang, L.; Wang, X.; De Corte, W. Systematic workflow for digital design and on-site 3D printing of large concrete structures: A case study of a full-size two-story building. *J. Build. Eng.* **2025**, *104*, 112370. [CrossRef]
15. Quah, T.K.N.; Tay, Y.W.D.; Lim, J.H.; Tan, M.J.; Wong, T.N.; Li, K.H.H. Concrete 3D printing: Process parameters for process control, monitoring and diagnosis in automation and construction. *Mathematics* **2023**, *11*, 1499. [CrossRef]
16. Ter Haar, B.; Kruger, J.; van Zijl, G. Off-site construction with 3D concrete printing. *Autom. Constr.* **2023**, *152*, 104906. [CrossRef]
17. Anton, A.; Reiter, L.; Wangler, T.; Frangez, V.; Flatt, R.J.; Dillenburger, B. A 3D concrete printing prefabrication platform for bespoke columns. *Autom. Constr.* **2021**, *122*, 103467. [CrossRef]
18. Cabibihan, J.J.; Gaballa, A.; Fadli, F.; Irshidat, M.; Mahdi, E.; Biloria, N.; Abdulrazak, H. A guided approach for utilizing concrete robotic 3D printing for the architecture, engineering, and construction industry. *Constr. Robot.* **2023**, *7*, 265–278. [CrossRef]
19. Puzatova, A.; Shakor, P.; Laghi, V.; Dmitrieva, M. Large-scale 3D printing for construction application by means of robotic arm and gantry 3D printer: A review. *Buildings* **2022**, *12*, 2023. [CrossRef]
20. Huang, S.; Xu, W.; Li, Y. The impacts of fabrication systems on 3D concrete printing building forms. *Front. Archit. Res.* **2022**, *11*, 653–669. [CrossRef]
21. Bello, N.D.; Memari, A.M. Comparative review of the technology and case studies of 3D concrete printing of buildings by several companies. *Buildings* **2022**, *13*, 106. [CrossRef]
22. Lowke, D.; Anton, A.; Buswell, R.; Jenny, S.E.; Flatt, R.J.; Fritschi, E.L.; Kloft, H. Digital fabrication with concrete beyond horizontal planar layers. *J. Cem. Concr. Res.* **2024**, *186*, 107663. [CrossRef]
23. Tiryaki, M.E.; Zhang, X.; Pham, Q.C. Printing-while-moving: A new paradigm for large-scale robotic 3D Printing. In Proceedings of the 2019 IEEE/RSJ International Conference on Intelligent Robots and Systems (IROS), Macau, China, 3–8 November 2019; pp. 2286–2291. [CrossRef]
24. Zhang, X.; Li, M.; Lim, J.H.; Weng, Y.; Tay, Y.W.D.; Pham, H.; Pham, Q.C. Large-scale 3D printing by a team of mobile robots. *Autom. Constr.* **2018**, *95*, 98–106. [CrossRef]
25. Izard, J.B.; Dubor, A.; Hervé, P.E.; Cabay, E.; Culla, D.; Rodriguez, M.; Barrado, M. Large-scale 3D printing with cable-driven parallel robots. *Constr. Robot.* **2017**, *1*, 69–76. [CrossRef]
26. Shanmugasundar, G.; Kalita, K.; Čep, R.; Chohan, J.S. Decision models for selection of industrial Robots—A comprehensive comparison of multi-criteria decision making. *Processes* **2023**, *11*, 1681. [CrossRef]
27. Hancu, O.; Rad, C.R.; Lapusan, C.; Brisan, C. Aspects concerning the optimal development of robotic systems architecture for waste sorting tasks. In Proceedings of the IOP Conference Series: Materials Science and Engineering, Melbourne, Australia, 5–16 September 2018; IOP Publishing: Bristol, UK, 2018; Volume 444, p. 052029. [CrossRef]
28. Goh, C.H. Analytic hierarchy process for robot selection. *J. Manuf. Syst.* **1997**, *16*, 381–386. [CrossRef]
29. Sivalingam, C.; Subramaniam, S.K. Cobot selection using hybrid AHP-TOPSIS based multi-criteria decision making technique for fuel filter assembly process. *Heliyon* **2024**, *10*, e26374. [CrossRef]
30. Khan, N.A.; Kumar, A.; Rao, N. An Insight into Multi-Criteria Decision Methods for the Selection of Robot: A Comprehensive Review. *SN Comput. Sci.* **2025**, *6*, 612. [CrossRef]

31. Lopes de Aquino Brasil, A.; Carmo Pena Martinez, A. A Systematic Review of Robotic Additive Manufacturing Applications in Architecture, Engineering, and Construction. *Buildings* **2025**, *15*, 3336. [CrossRef]
32. Yabanigül, M.N.; Gulec Ozer, D. Exploring Architectural Units Through Robotic 3D Concrete Printing of Space-Filling Geometries. *Buildings* **2024**, *15*, 60. [CrossRef]